Luminescence Thermochromism in Dicyanoargentate(I) Ions Doped in Alkali Halide Crystals†

Manal A. Rawashdeh-Omary,‡,§ Mohammad A. Omary,‡,§ George E. Shankle,|| and Howard H. Patterson*,‡

Department of Chemistry, University of Maine, Orono, Maine 04469, and Department of Chemistry, Angelo State University, San Angelo, Texas 76909

Received: February 11, 2000; In Final Form: April 17, 2000

Single crystals of $[Ag(CN)_2^-]$/NaCl and $[Ag(CN)_2^-]$/KCl show luminescence spectra that change drastically with temperature. The major luminescence band at 12 K is a UV emission at about 315 nm. Blue-green emissions in the 400−520 nm region appear upon an increase in temperature to 80 K. A further increase in temperature results in the disappearance of the blue-green emissions and the appearance of a high-energy UV emission at about 290 nm. The color changes are reversible and represent a new example of luminescence thermochromism. A kinetic model is proposed to show the radiative and nonradiative pathways at different temperatures. Highly resolved emission spectra are obtained upon a careful selection of the excitation wavelength. Individual peaks within the resolved emission bands are attributed to different geometrical isomers of a given $*[Ag(CN)_2^-]_n$ cluster in the alkali halide lattices. The wide range of luminescence energy, the strong luminescence at ambient temperature, and the control of the profile of the emission spectra by controlling the excitation wavelength are desired properties for the design of new solid-state photonic devices based on the Ag(I) luminescence.

Introduction

Coordination compounds of the d^{10} monovalent ions of group 11 have been the subject of increasing attention in the last 25 years.[1−3] This attention has been stimulated by the desire to understand some fundamental issues in chemistry such as closed-shell metal−metal bonding, as well as the use of these compounds in many technological applications. Much of the early work in this field has focused on Cu(I) species due to many interesting luminescence properties of some Cu(I) tetranuclear clusters. For example, Hardt et al. have reported that the clusters $Cu_4L_4X_4$ (L = aromatic amine, X = halide) reversibly alter their luminescence color with temperature.[4] This interesting phenomenon (called luminescence thermochromism) has been elucidated by Ford et al. in a series of articles that aimed at the assignment of the two luminescence bands whose relative intensities change with temperature.[5] Interest in gold(I) compounds has been increasing in recent years, partially because of the tremendous attention given to the relationship between the electronic properties of gold(I) compounds to *aurophilic attraction*,[6] namely, ground-state Au−Au interactions. Recently, analogous *argentophilic attraction* has been reported in Ag(I) coordination compounds.[7] Photoluminescence studies of the dicyanoargentate(I) ions have pointed out that excited-state Ag−Ag interactions are much stronger than the corresponding ground-state interactions.[8,9]

Examples of the use of Cu(I) materials in technological applications include the photosensitization of water splitting via energy and electron transfer pathways,[10] photocatalysis,[11] and the potential use of Cu(I) in oxide materials in tunable solid-state laser materials in the UV.[12] Gold(I) compounds have been suggested for applications such as biosensors,[13] photocatalysts,[14] drugs for rheumatoid arthritis,[15] and optical sensors for volatile organic compounds.[16] Applications of Ag(I) materials include the use of silver halides as photographic materials[17] and as optical fibers in the mid-IR region,[18] and the use of silver(I) oxides as photocatalysts,[19] conductors, semiconductors, and photoconductors.[1,20−22]

We report herein a study of the temperature-dependent photoluminescence properties of single crystals of alkali halides doped with dicyanoargentate(I) ions. An earlier study in our laboratory has suggested the formation of luminescent exciplexes in $[Ag(CN)_2^-]$/KCl mixed crystals.[8] Exciplex formation is well known in organic compounds[23] but less common in inorganic compounds.[24] The $*[Ag(CN)_2^-]_n$ exciplexes that we have reported in pure[9] and mixed[8] crystals of the dicyanoargentates(I) are metal−metal bonded and represent a new class of exciplexes in which the exciplex bond[24b] is between the same type of atoms (homoatomic metal−metal bonded exciplexes). Several emission bands appear in the spectra of alkali halide crystals that are doped with $[Ag(CN)_2^-]$ ions, giving rise to an interesting optical phenomenon called *exciplex tuning*. We have reported that the emission energies and intensities can be *tuned* by changing the excitation wavelength (site-selective excitation)[8] and by varying the dopant concentration.[25] Changing the excitation wavelength controls which $[Ag(CN)_2^-]_n$ oligomer is excited and, hence, which $*[Ag(CN)_2^-]_n$ exciplex emits light, because different oligomers have different energy gaps.[8] On the other hand, changing the dopant concentration increases the statistical probability of longer oligomers (e.g., trimers versus

†This is part 3 of a series entitled Luminescent Homoatomic Exciplexes in Dicyanoargentate(I) Ions Doped in Alkali Halide Crystals. Parts 1 and 2 of this series have been published earlier: Omary, M. A.; Patterson, H. H. *J. Am. Chem. Soc.* **1998**, *120*, 7696. Omary, M. A.; Hall, D. R.; Shankle, G. E.; Siemiarczuck, A.; Patterson, H. H. *J. Phys. Chem. B* **1999**, *103*, 3845.

|| Angelo State University.

‡ Present address: Department of Chemistry, Texas A&M University, College Station, TX 77843.

10.1021/jp000563x CCC: $19.00
Published on Web 06/10/2000

dimers), which leads to stronger emission intensities for the trimer bands.[25] In this article we report that *exciplex tuning* can also be achieved by temperature variation in two types of mixed crystals. The formation of dicyanoargentate(I) exciplexes in [Ag-$(CN)_2^-$]/NaCl is studied herein in comparison with [$Ag(CN)_2^-$]/KCl in order to illustrate the effect of the host crystal on exciplex formation. The implications of exciplex tuning on the design of new solid-state photonic devices are discussed.

Experimental Section

Single crystals of [$Ag(CN)_2^-$]/KCl and [$Ag(CN)_2^-$]/NaCl were grown by slow evaporation at ambient temperature of aqueous solutions that are ~2 M in the alkali halide and that contain trace amounts (<0.05 M) of K[$Ag(CN)_2$] and (NaCN; AgCN), respectively. The silver content was determined by atomic absorption spectroscopy using a Varian SpectrAA-20 spectrophotometer with an air-acetylene flame and a Ag analytical lamp operating at 328.1 nm. The standards for the atomic absorption analysis were prepared using Aldrich 1000 ppm Ag standard in 1% HNO_3. Atomic absorption measurements were run in triplicate for each sample of crystals harvested at the same time. The single crystals in this study were characterized by FTIR, and all crystals show infrared bands in the region of the C−N stretching frequencies of typical [$Ag(CN)_2^-$] species (2000−2200 cm^{-1}).

Steady-state photoluminescence spectra were recorded with a Model QuantaMaster-1046 fluorescence spectrophotometer from Photon Technology International, PTI. The instrument is equipped with two excitation monochromators and a 75 W xenon lamp. The excitation spectra were corrected for spectral variations in the lamp intensity using the standard quantum counter method[26] by dividing the raw data by the excitation spectrum of rhodamine B (λ_{em} = 635 nm). The spectra were recorded for single crystals with high optical purity as a function of temperature between 12 K and ambient temperature. Liquid helium was used as the coolant in a Model LT -3-110 Heli-Tran cryogenic liquid transfer system from Air Products equipped with a temperature controller. Excited-state lifetime measurements were carried out with a QuantaMaster-2 system from PTI utilizing a microsecond Xe flash lamp and a gated microsecond detector.

Results

1. Luminescence Properties at 80 K. The single crystals of [$Ag(CN)_2^-$]/NaCl studied have 0.31 wt %Ag (0.17 mol %). These crystals have photoluminescence spectra that are dependent on the excitation wavelength and temperature. The luminescence characteristics of [$Ag(CN)_2^-$]/NaCl crystals are best described by presenting the data at 80 K first and then discussing the temperature dependence. This is because the intensities for all [$Ag(CN)_2^-$] luminescence bands are significant at 80 K, while at higher or lower temperatures some of these bands are absent. Figure 1 illustrates the tunable emission of [$Ag(CN)_2^-$]/NaCl at 80 K as a function of excitation wavelength. Four major emission bands are evident with maxima at ca. 295, 325, 420, and 500 nm (labeled in Figure 1 as A, B, C, and D, respectively).[27a] The relative intensity of each band is dependent on the excitation wavelength, as Figure 1 clearly illustrates. Figure 2 shows the corrected excitation spectra of [$Ag(CN)_2^-$]/NaCl at 80 K monitoring the emission at wavelengths that correspond to each emission band. The characteristic excitation wavelengths are located at ca. 220−235, 280−290, and 245−270 nm for bands A, B, and C, respectively. The excitation profile for band D is similar to the one for band C. Table 1 summarizes the luminescence data for both [$Ag(CN)_2^-$]/NaCl and [$Ag(CN)_2^-$]/KCl.

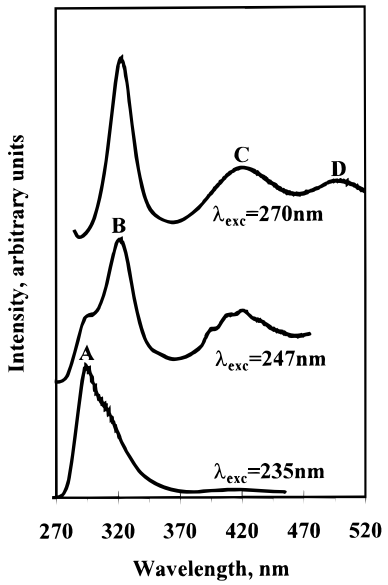

Figure 1. Emission spectra of [$Ag(CN)_2^-$]/NaCl at 80 K as a function of excitation wavelength.

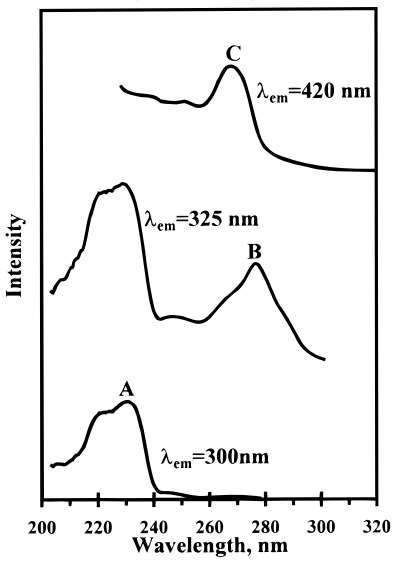

Figure 2. Corrected excitation spectra of [$Ag(CN)_2^-$]/NaCl at 80 K monitoring the emission at wavelengths that correspond to bands A−D.

TABLE 1: Assignment of the Emission Bands Observed in [$Ag(CN)_2^-$]/NaCl and [$Ag(CN)_2^-$]/KCl Crystals

band	λ_{max}^{em}, nm	λ_{max}^{exc}, nm	lifetime, μs^a	assignment
A	285−300	225−250	2.8[b] (5.3)[c]	*$[Ag(CN)_2^-]_2$ (excimers)
B	310−360	270−290	6.5[b]	*$[Ag(CN)_2^-]_3$ (angular)
C	390−430	250−270	27.4[b] (39%) 64.4[b] (61%)	*$[Ag(CN)_2^-]_3$ (linear)
D	490−530	300−360		*$[Ag(CN)_2^-]_n$ (delocalized exciplexes)

[a] Lifetime measurements have been determined for the P2 crystal of [$Ag(CN)_2^-$]/KCl. [b] Data from ref 25 at 77 K. [c] Data from this work at ambient temperature.

2. Luminescence Thermochromism. A rather interesting temperature dependence has been obtained for the luminescence of [$Ag(CN)_2^-$]/NaCl single crystals. Figure 3 shows the emission spectra of [$Ag(CN)_2^-$]/NaCl as a function of temperature and excitation wavelength. The excitation wavelengths are selected

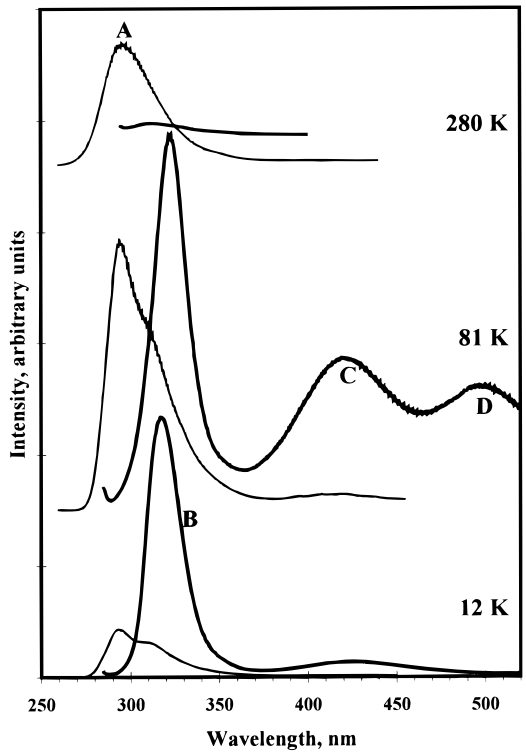

Figure 3. Emission spectra of $[Ag(CN)_2^-]$/NaCl as a function of temperature and excitation wavelength. Thin and thick curves represent spectra obtained with excitation wavelengths of 235 and 270 nm, respectively. Intensities are comparable between spectra at the same temperature but not comparable between spectra at different temperatures.

as 235 and 270 nm for the temperature-dependent spectra in Figure 3. These wavelengths are selected to best illustrate the high-energy bands (A and B) and the low-energy bands (C and D), respectively. At 12 K, the high-energy bands have greater intensities than the low-energy bands. Both the UV bands A and B have strong intensities, while the blue band C is present but weak at 12 K. The green band D, on the other hand, is absent at 12 K. As the temperature is increased from 12 K, the relative intensities of the low-energy bands (C and D) increase until 80 K and decrease thereafter. In fact, all four $[Ag(CN)_2^-]$ luminescence bands (A−D) are strong at 80 K. Band D is observed only near 80 K and becomes quenched at higher or lower temperatures. The high-energy bands display strong intensities at all temperatures. However, among the two high-energy bands, the intensity ratio of band A to band B increases with an increase in temperature over the whole temperature range between 12 K and ambient temperature. The positions of the $[Ag(CN)_2^-]$ luminescence bands are virtually temperature independent (within 5 nm).

Three mixed crystals of $[Ag(CN)_2^-]$/KCl with varying Ag content have been studied. We refer to the $[Ag(CN)_2^-]$/KCl crystals with wt % Ag of 0.17, 2.7, and 4.3 as P1, P2, and P3, respectively.[27b] Although all three crystals show luminescence thermochromism, the most dramatic results have been obtained for P3. Figure 4 shows the emission spectra of P3 as a function of temperature. At ambient temperature only band A is observed. Cooling to 77 K results in a virtual disappearance of band A concomitant with the appearance of a strong emission due to the lower-energy band C. Upon further cooling to 12 K, the strongest emission becomes due to the higher-energy band B.

Another interesting aspect of the photoluminescence properties of the $[Ag(CN)_2^-]$/NaCl and $[Ag(CN)_2^-]$/KCl single crystals

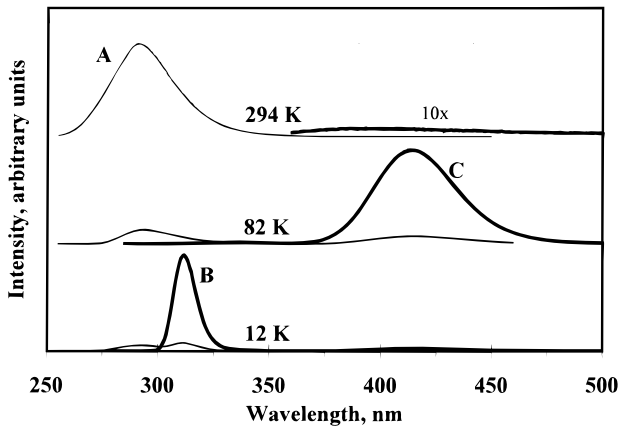

Figure 4. Emission spectra of a KCl/$KAg(CN)_2$ crystal (P3) as a function of temperature and excitation wavelength. Thin and thick curves represent spectra obtained with excitation wavelengths of 235 and 270 nm, respectively. Intensities are comparable between spectra at the same temperature but not comparable between spectra at different temperatures.

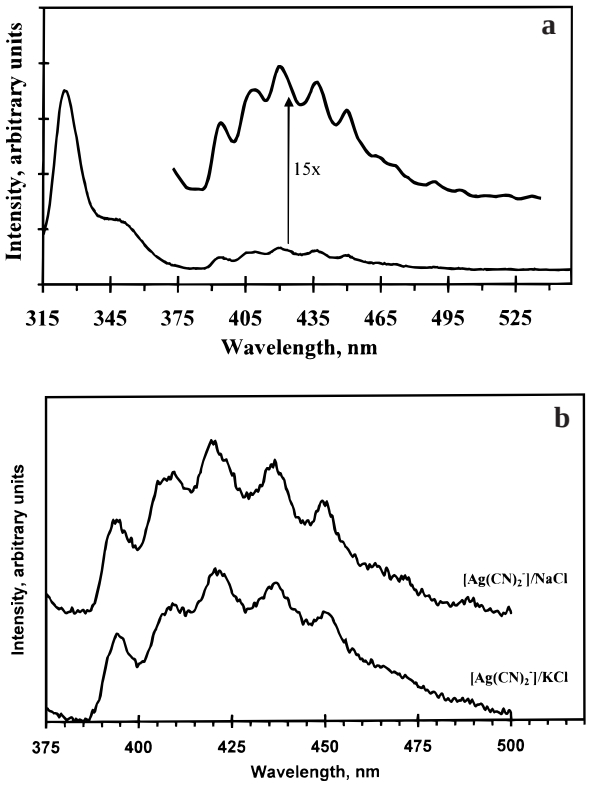

Figure 5. (a) Emission spectrum of a $[Ag(CN)_2^-]$/NaCl single crystal at 12 K with $\lambda_{exc} = 293$ nm showing high resolution. (b) Emission spectra of a KCl/$KAg(CN)_2$ crystal (P3) at 81 K (bottom) and a $[Ag(CN)_2^-]$/NaCl single crystal at 12 K (top). The excitation wavelength is 293 nm in both spectra.

is the observation of highly resolved spectra upon a careful selection of the excitation wavelength. This resolution is especially high at low temperatures. As a representative example of the highly resolved spectra, Figure 5a shows the emission spectrum of a $[Ag(CN)_2^-]$/NaCl single crystal at 12 K with $\lambda_{exc} = 293$ nm. Band B has two resolved peaks at 325 and 350 nm, while at least seven resolved peaks appear within the envelop of band C. Figure 5b illustrates that the resolution in the emission spectra of the dicyanoargentates(I) occurs also in $[Ag(CN)_2^-]$/KCl-doped crystals. The profile of the structured emission of band C is similar for $[Ag(CN)_2^-]$/KCl and [Ag-

$(CN)_2^-$]/NaCl crystals. Figure 5b illustrates that the same number of peaks within the structured band C are obtained at virtually the same energies for both crystals.

Discussion

1. Temperature Dependence of the Luminescence Bands. Since the [$Ag(CN)_2^-$] monomer is not luminescent,[8] all dicyanoargentate(I) emission bands must be due to silver−silver interactions. An increase in metal−metal interactions decreases the energy of the absorption and emission bands for [$Ag(CN)_2^-]_n$ species (see ref 8 for details). On the basis of this discussion, we provide in Table 1 the assignment of all emission bands observed in the [$Ag(CN)_2^-$]/NaCl and [$Ag(CN)_2^-$]/KCl crystals studied herein.

The aforementioned temperature behavior illustrates strong "luminescence thermochromism" in dicyanoargentates(I). This interesting phenomenon was first reported for coordination compounds in tetranuclear Cu(I) clusters by Hardt et al.,[4] and these compounds have attracted considerable attention in recent years.[5] The results herein illustrate that this phenomenon might be general for coordination compounds of monovalent ions of the coinage metals.[28] Luminescence thermochromism in Cu(I) clusters such as $Cu_4I_4(py)_4$ is indicated by the appearance of emissions with markedly different visible colors at different temperatures.[4] Some temperature changes in the [$Ag(CN)_2^-$] systems occur between emission bands that are in the ultraviolet region (e.g., bands A and B), whereas all luminescence bands for the Cu(I) clusters are in the visible region, which results in more marked color changes to the naked eye in the Cu(I) clusters compared to the [$Ag(CN)_2^-$] systems. From a scientific point of view, however, the changes in the study herein are more dramatic. In the present study a major emission band at a certain temperature is virtually absent at a different temperature (for example see band C in Figure 4). This is not the case in most solids of the Cu(I) clusters, in which the low-energy band remained stronger than the high-energy band even at low temperatures at which the high-energy band becomes prominent.[4] Moreover, the temperature changes in the present study occur for four emission bands, as opposed to only two emission bands for the Cu(I) clusters.

Multiple temperature-dependence trends have been observed for the luminescence spectra of each crystal studied herein. Therefore, more than one factor must be responsible for the temperature dependence observed. We shall discuss four possibilities that are normally used to explain changes in luminescence bands as a result of temperature variation. The first possibility is that varying the temperature results in a change in Ag−Ag distances. Several studies have reported red shifts of the luminescence bands of low-dimensional layered compounds upon cooling as a result of the thermal reduction of metal−metal distances.[4d,9,29−34] However, in such cases relatively small red shifts within the same luminescence band are normally observed upon cooling. For example, Tl[$Ag(CN)_2$] has an emission band with a shape and energy similar to band C in Table 1.[9,30] The emission peak of Tl[$Ag(CN)_2$] undergoes a red shift of only 500 cm^{-1} upon cooling single crystals of the compound from 195 to 10 K,[9,30] as a result of the thermal reduction of the Ag−Ag distance within the cluster responsible for the emission band.[35] Layered compounds that exhibit red shifts in their luminescence bands upon cooling normally exhibit a corresponding decrease of metal−metal distances by no more than 0.1 Å when the temperature is decreased from ambient temperature to near liquid helium temperatures.[32,34−36] In Figures 3 and 4, however, we observe the disappearance of one band and the appearance of another, so this cannot be explained by the expected small reductions in the Ag−Ag distance. Therefore this possibility is ruled out.

The second possibility is the presence of major structural changes such as phase transitions. Such changes may lead to different structures of the luminescent [$Ag(CN)_2^-]_n$ ions at different temperatures. Therefore, the cluster size (n) and/or the geometry of a given cluster may be altered as a result of temperature variation, which leads to corresponding changes in the relative intensities of the different luminescence bands. This possibility cannot be proved or disproved in mixed crystals such as those studied herein because of the difficulty in obtaining direct structural data for such crystals. However, an analogy can be made with pure crystals of the dicyanoargentate(I), some of which exhibit luminescence bands that have a temperature behavior similar to the one herein.[37] For example, single crystals of $K_2Na[Ag(CN)_2]_3$ display a change in the relative intensities of bands B and C above and below 80 K (similar to the trend in Figure 4).[37] Recent neutron diffraction data versus temperature indicate the absence of phase transitions in $K_2Na[Ag(CN)_2]_3$ near 80 K.[36] Therefore, it is not likely that phase transitions are responsible for the trends shown in Figures 3 and 4.

The third possibility is that the luminescence bands may be fluorescence and phosphorescence and each component has a different temperature dependence from the other. We rule out this possibility because our data indicate that all luminescence bands observed for [$Ag(CN)_2^-$]/KCl have excited-state lifetimes with microsecond values (Table 1). Therefore, all luminescence bands A−D are assigned to phosphorescence of the relevant *[$Ag(CN)_2^-]_n$ triplet exciplexes rather than fluorescence.

The mechanism responsible for the temperature behavior of the luminescence bands in this study involves the transfer of excitation energy between excitons characteristic of clusters responsible for individual emission bands. Nonradiative energy transfer processes are known to be strongly dependent upon temperature. An increase in the intensity ratio of the LE/HE luminescence bands upon increasing the temperature is a typical behavior of "normal" energy transfer processes due to the thermal nature of such processes. This is illustrated by the increase in the relative intensities of the blue-green emissions in [$Ag(CN)_2^-$]/NaCl at the expense of the UV emissions as the temperature is increased from 12 to 80 K (Figure 3). On the other hand, the reduction in the intensity ratio of the LE/HE bands as temperature is increased between 80 K and ambient temperature does not follow this "normal" trend. "Back transfer" processes must, therefore, be responsible for this behavior of [$Ag(CN)_2^-$]/NaCl and [$Ag(CN)_2^-$]/KCl above 80 K. Back transfer refers to energy transfer from a lower-energy level to a higher-energy level. In this case, back transfer proceeds from the energy levels characteristic of the lower-energy bands C and D to those of the higher-energy bands A and B. Back transfer is not favorable from thermodynamic considerations because it is an endothermic process. In contrast, a "normal" energy transfer process occurs from a higher-energy level to a lower-energy level and is, thus, exothermic. Therefore, back transfer processes require much higher activation energies than normal energy transfer processes. Consequently, such back transfer mechanisms become important at high temperatures so as to surmount these high activation energies. For example, Kambli and Güdel have reported that back transfer processes proceed at higher temperature than those needed for "normal" energy transfer processes in antiferromagnets such as $CsMnX_3$ and $RbMnX_3$ (X = Cl, Br).[38] A similar result has been reported recently for Y[$Au(CN)_2]_3$.[39] The efficiencies of back transfer

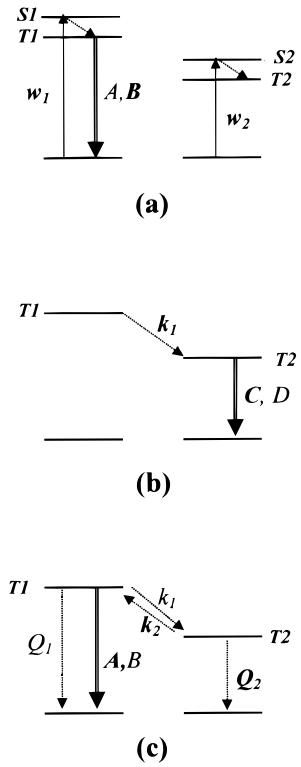

Figure 6. Kinetic model showing the major radiative and nonradiative pathways responsible for luminescence thermochromism in the dicyanoargentates(I). The major pathways are depicted at 12 K (a). Also shown are additional pathways that occur as the temperature is increased between 12 and 80 K (b) and between 80 K to ambient temperature (c). Solid single lines represent absorption, double lines represent emission, and dashed lines represent nonradiative processes. The symbols "*w*", "*k*", and "*Q*" represent rates of excitation, energy transfer, and quenching pathways, respectively. The symbols "*S*" and "*T*" represent singlet and triplet states, respectively.

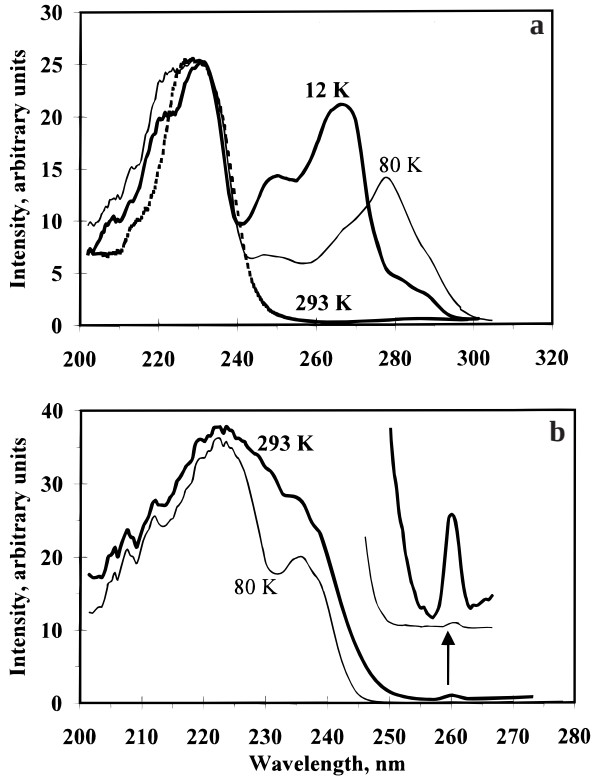

Figure 7. (a) Corrected excitation spectra of $[Ag(CN)_2^-]$/NaCl versus temperature monitoring the band B emission. (b) Corrected excitation spectra of $[Ag(CN)_2^-]$/KCl versus temperature monitoring the band A emission.

processes also increase in the presence of phonon assistance. The high vibrational frequency of the cyanide groups (~2150 cm^{-1}) provides strong phonon assistance for such back transfer processes in the $[Ag(CN)_2^-]$/NaCl and $[Ag(CN)_2^-]$/KCl crystals.

In a recent article, we have demonstrated that individual luminescence bands of $[Ag(CN)_2^-]$/KCl are observed as a result of direct excitation of a given $[Ag(CN)_2^-]_n$ cluster as well as energy transfer from other $[Ag(CN)_2^-]_n$ clusters.[25] On the basis of time-resolved emission spectra at 77 K, it was concluded that energy transfer proceeds from excitons characteristic of band A (as donors) to excitons responsible for band C (as acceptors). The relative importance of direct excitation versus energy transfer is a function of temperature. In the absence of major structural changes, the direct excitation pathway should not be affected by temperature variation because this pathway is controlled by the statistical probabilities of the different $[Ag(CN)_2^-]_n$ clusters. Energy transfer pathways, in contrast, are strongly dependent on temperature. In Figure 6, we propose a simplified kinetic model in an attempt to explain the complicated temperature trends of the luminescence spectra in the present study. Although four luminescence bands are displayed by the mixed crystals in this study, the model in Figure 6 shows the electronic states of two species only for simplicity. Therefore, the clusters responsible for the HE bands A and B are collectively represented by the electronic states on the left, while the clusters responsible for the LE bands C and D are represented by the electronic states on the right.[40]

At very low temperatures (e.g., 12 K), energy transfer processes are minimized and, hence, the luminescence is controlled only by direct excitation processes. We have established in ref 25 that the statistical probability is higher for $[Ag(CN)_2^-]_n$ clusters with a smaller number of ions (e.g., with $n = 2$) than those with a larger number of ions (e.g., with $n = 3$) in the face-centered cubic alkali halide lattices. Therefore, $w_1 \gg w_2$ in Figure 6a. This explains the domination of the HE bands at 12 K (Figures 3 and 4). Upon increasing the temperature between 12 and 80 K, "normal" energy transfer processes become significant (k_1 in Figure 6b). Consequently, the relative intensities of the LE bands increase (Figures 3 and 4). As the temperature is increased further toward ambient temperature, two additional nonradiative processes compete with k_1 (Figure 6c): "back" energy transfer (k_2) and nonradiative deexcitation (Q_1 and Q_2). It is expected that $Q_1 \ll Q_2$ by virtue of the energy-gap law.[41] Moreover, the complete quenching of the LE emission bands C and D at ambient temperature (Figures 3 and 4) suggests that $(k_2 + Q_2) \gg k_1$. Both of these factors lead to a decrease of the relative intensity of the LE band concomitant with an increase in the relative intensity of the HE bands upon increasing the temperature from 80 K toward ambient temperature.

Analysis of the luminescence excitation spectra provides invaluable information about the mechanism of the excited-state processes and allows us to check the validity of the kinetic model proposed in Figure 6. Figure 7a shows the excitation spectra of a $[Ag(CN)_2^-]$/NaCl crystal versus temperature monitoring the band B emission. The lower-energy region of the excitation spectra ($\lambda > 240$ nm) represents direct excitation of band B oligomers, while the higher-energy region ($\lambda < 240$ nm) represents energy transfer from band A excitons (see Table 1 and Figure 2). According to Figure 7a, the relative intensity of the lower-energy peaks decreases with an increase in temperature from 12 to 80 K to 293 K. That is, direct excitation

becomes less important and "normal" energy transfer from the higher-energy band A to the lower-energy band B becomes a more dominant mechanism at high temperatures. According to the discussion above, "back" energy transfer becomes important at temperatures above 80 K. Excitation spectra of band A versus temperature are in support of this hypothesis. Figure 7b shows the excitation spectra of a $[Ag(CN)_2^-]$/KCl crystal versus temperature monitoring the band A emission. It is noticed that the relative intensity of the peak at ~260 nm is much higher at ambient temperature than at 80 K. Since this peak is due to energy transfer from the lower-energy band C to the higher-energy band A, Figure 7b provides evidence that back transfer is a valid mechanism between 80 K and ambient temperature. It is noted that the relative intensities of the higher-energy peaks are stronger in both Figures 7a and 7b. This is due to the higher statistical probability of the dimers than the trimers in the alkali halide lattice.[25] Therefore, we conclude that energy transfer is the dominant mechanism for the observation of the luminescence characteristic of trimer oligomers at all temperatures and direct excitation becomes less and less important with an increase in temperature. Meanwhile, direct excitation is the dominant mechanism for the observation of the luminescence characteristic of dimer oligomers at all temperatures and that back energy transfer becomes more and more important with an increase in temperature.

2. Kinetic Processes. Excited state lifetime measurements have been determined for the luminescence bands of the dicyanoargentate(I) luminescence bands at 77 K and at ambient temperature (Table 1). The results can be related to the kinetic model shown in Figure 6. In this analysis we shall use the lifetimes for bands A and C in relation to the states in Figure 6 characteristic of the HE and LE emissions, respectively. According to the model in Figure 6, the time dependence of the A and C emissions at 77 K can be described by eqs 1 and 2, respectively (see ref 25 for mathematical details):

$$N_A(t) = N_A(0)\exp(-\{k_A + k_1\}t) \quad (1)$$

$$N_C(t) = N_A(0)[k_1/(k_C^{(1)} - k_A - k_1)][\exp(-\{k_A + k_1\}t) - \exp(-k_C^{(1)}t)] + N_C(0)\exp(-\{k_C^{(2)}\}t) \quad (2)$$

where $N_A(t)$ and $N_C(t)$ represent the population of the excited states characteristic of bands A and C, respectively, while k_A and k_C represent the radiative decays of bands A and C, respectively.

According to eq 1, band A decays exponentially with only one lifetime component, in agreement with the experimental results ($\tau_A = 2.8\ \mu$s; see Table 1). The mechanism depicted in Figure 6, therefore, accurately describes the time dependence of band A emission at 77 K. On the other hand, eq 2 predicts that band C has a rise time and two decay time components. The rise time component of the band C emission should be equal in magnitude to the decay time of band A, according to eq 2. One of the two decay components of band C is due to the feeding mechanism from band A excitons ($\tau = 1/k_C^{(1)}$), and the other component is due to direct excitation ($\tau = 1/k_C^{(2)}$). Experimentally, band C has a virtual zero rise time and a dual lifetime decay with a slow component $\tau_C^{(1)} = 64\ \mu$s, due to energy transfer from A, and a fast component $\tau_C^{(2)} = 27\ \mu$s, due to direct excitation. The magnitude of the fast component is significantly longer than the decay time of band A (2.8 μs). Therefore, the rate-determining step in the short time domain for band C is direct excitation, which explains the absence of a rise time experimentally.

TABLE 2: Vibrational Level Analysis of the Resolved Peaks in the Luminescence Band between 380 and 480 nm in Figure 5a[a,b]

ν, cm^{-1}	$\Delta\nu$, cm^{-1}	$\nu-\nu_0$, cm^{-1}
2.54×10^4		0
2.44×10^4	9.31×10^2	9.31×10^2
2.38×10^4	6.40×10^2	1.57×10^3
2.29×10^4	8.74×10^2	2.44×10^3
2.22×10^4	6.89×10^2	3.13×10^3
2.16×10^4	6.25×10^2	3.76×10^3
2.12×10^4	4.58×10^2	4.22×10^3
average $\Delta\nu$	703 ± 174 cm^{-1}	
% std dev	24.8	

[a] The electronic origin is assumed to be the highest-energy peak (2.54×10^4 cm^{-1}). [b] Notation used in this table: ν_0, wavenumber of the electronic origin; $\Delta\nu$, spacing between neighboring peaks; $\nu-\nu_0$, wavenumber difference between each peak and the electronic origin.

At ambient temperature, one needs only to derive the time dependence of the band A emission because the lower-energy bands are quenched. Considering the additional processes shown in Figure 6c and assuming that $w_1 \gg w_2$, we obtain

$$N_A(t) = (w/[k^+ - k^-])[(k^+ + k_2 + Q_2)\exp(k^+t) - (k^- + k_2 + Q_2)\exp(k^-t)] \quad (3)$$

where $k^\pm$ are constants given by eq 4:

$$2k^\pm = -(k_A + k_1 + k_2 + Q_1 + Q_2) \pm [(k_A + k_1 - k_2 + Q_1 - Q_2)^2 + 4k_1k_2]^{1/2} \quad (4)$$

Equation 3 suggests that a monoexponential lifetime decay should exist for band A at room temperature, in agreement with the experimental result ($\tau_A = 5.3\ \mu$s; see Table 1). However, the equation also predicts the existence of a rise time, which we have not seen with the gated microsecond detector. Finally, the increase in the lifetime of band A from 2.8 μs at 77 K to 5.3 μs at ambient temperature is in support of the kinetic model, which proposes the presence of the back transfer mechanism in addition to direct excitation.

3. Analysis of Fine Structure. Another interesting feature of the dependence of the luminescence on the excitation wavelength is illustrated in Figure 5a for $[Ag(CN)_2^-]$/NaCl. A highly resolved emission spectrum of this system is obtained when certain excitation wavelengths are selected (293 nm in Figure 5a), especially at low temperatures. Site-selective spectroscopy is a well-known method that is used to improve the resolution of the emission spectra.[42−44] The resolved peaks are normally characterized as vibronic structure that shows a progression of some vibrational modes in the luminescent species. This progression is normally analyzed by the classical Franck−Condon method or by the time-dependent theory of electronic and Raman spectroscopies, to gain information about the assignment of the excited state.[44] However, the appearance of structured emission in Figure 5 is unusual and is unlikely due to vibronic structure for two reasons. First, the dicyanoargentate(I) emission has been characterized as an exciplex emission.[8] Excimer and exciplex emissions are known to have structureless luminescence bands.[23] Second, the spacing between the individual peaks that appear in Figure 5 does not correspond to any dicyanoargentate(I) vibrational mode.

Table 2 shows a vibronic level analysis of the individual peaks that appear in the luminescence band that extends between 380 and 480 nm in Figure 5. In this analysis we assume that the

electronic origin (ν_0) is 2.54×10^4 cm^{-1}, which corresponds to the highest-energy peak (394.0 nm). The resolved peaks have an average separation ($\Delta\nu$) of 703 ± 174 cm^{-1}. The most prominent vibrational mode for the [Ag(CN)$_2^-$] ion ($D_{\infty h}$) is the C−N symmetrical stretch near 2150 cm^{-1}.[45] The average $\Delta\nu$ value of 703 cm^{-1} is much lower than ν_{C-N}. Meanwhile, the other [Ag(CN)$_2^-$] vibrational modes have energies below 400 cm^{-1} (e.g., Ag−C stretching and the C−N bending modes occur near 360 and 250 cm^{-1}, respectively). Therefore, the 703 cm^{-1} value for the $\Delta\nu$ value is much higher than the energies of these modes. Vibronic progressions such as the "missing mode effect"[44] have been reported in the literature in coordination compounds such as W(CO)$_5$(pyridine)[44b] and K$_2$[PtCl$_6$].[44c] However, for such progressions to occur a combination is required between at least two vibrational modes that are close in frequency to each other. The missing mode will usually have an intermediate frequency.[44] For a missing mode effect to be responsible for the structure in Figure 5, a combination of the ν_{C-N} mode at 2150 cm^{-1} and the low-frequency modes (<400 cm^{-1}) must exist because the $\Delta\nu$ value of 703 cm^{-1} in Table 2 is an intermediate value. The large difference in frequency between the ν_{C-N} mode and the low-frequency modes of [Ag(CN)$_2^-$] precludes any coupling by the missing mode effect. Another unusual progression that has been reported is the "beat frequency" (e.g., in ruthenocene),[44d] which corresponds to the energy difference between two modes. Obviously, the structure in Figure 5 cannot be explained by a beat frequency because no two normal modes of [Ag(CN)$_2^-$] differ by 703 cm^{-1}.

The possibility that the structure in Figure 5 is caused by F-center progressions (due to the alkali halide hosts) is ruled out because Figure 5b illustrates that the structure observed is virtually independent of the type of alkali halide host (NaCl or KCl). In addition, the spacings observed herein do not correspond to the phonon energies of F-centers in NaCl or KCl. The effective phonon energies of F-center emissions in KCl and NaCl have been reported as 0.0188 eV (151 cm^{-1}) and 0.0243 eV (196 cm^{-1}), respectively.[46] Obviously, the spacings observed in Figure 5 and Table 2 have much higher frequencies than these values for F-centers and, besides, have virtually the same values for both NaCl and KCl, unlike the case for F-centers in these crystals.

We propose that the different peaks within the same luminescence band correspond to different geometrical isomers of the [Ag(CN)$_2^-$]$_n$ cluster that is responsible for the structured luminescence band. This is valid for both bands B and C, as illustrated in Figure 5a. A statistical distribution analysis reveals that the [Ag(CN)$_2^-$]$_3$ trimer has more than 25 possible geometrical isomers when doped in a KCl lattice.[8] The same argument applies for [Ag(CN)$_2^-$]$_3$ in NaCl because both KCl and NaCl have the same space group. In our study of a variety of [Ag(CN)$_2^-$] species, we have observed the same type of structure shown in Figure 5 using certain excitation wavelengths.[37] The energies of individual peaks within the same emission band are virtually unaffected by changing the host lattice, the dopant concentration, or the temperature. These factors have affected only the resolution and sometimes the relative intensities of the resolved peaks, but not their energies.[37] These experimental observations are in support of the aforementioned assignment of the structured emission. Electronic structure calculations are also in support of this assignment. Density-functional theory (DFT) calculations were carried out at the B3LYP level using the LANL2DZ basis set.[8] The results show that the energy of a [Ag(CN)$_2^-$]$_2$ dimer is strongly dependent on the dihedral angle between the two ions. Variation of the dihedral angle between 0° and 90° (15° increments) resulted in a stepwise reduction in the total electronic energy with a total stabilization of 23.3 kJ/mol for the 90° (staggered) isomer relative to the 0° (eclipsed) isomer. Further calculations have indicated that the HOMO−LUMO gaps for [Ag(CN)$_2^-$]$_2$ and [Ag(CN)$_2^-$]$_3$ models are sensitive to the geometry and dihedral angles.[8] For example, the HOMO−LUMO gap for the staggered linear trimer is 2.18×10^3 cm^{-1} lower in energy than that for the corresponding eclipsed isomer. Meanwhile, the eclipsed linear trimer has a HOMO−LUMO gap that is 1.37×10^3 cm^{-1} lower in energy than that for the eclipsed angular trimer. Therefore, one would expect different absorption and emission energies for the variety of [Ag(CN)$_2^-$]$_3$ isomers that do exist in the alkali halide lattice, with no particular constant energy separation between the individual peaks representing these isomers.

4. Effect of the Host Crystal. We wish to discuss in this section the similarities and differences in the luminescence behavior of the dicyanoargentate(I) ions in the NaCl-doped crystals versus the KCl-doped crystals. An example of the sensitivity of the [Ag(CN)$_2^-$] luminescence to the host crystal is the appearance of the low-energy band D near 500 nm. This band appears with a reasonably strong intensity in the luminescence spectrum of [Ag(CN)$_2^-$]/NaCl crystals (Figure 3) but is virtually absent in analogous [Ag(CN)$_2^-$]/KCl crystals with similar or even higher dopant concentration (Figure 4). The dicyanoargentate(I) emission near 500 nm is assigned to delocalized exciplexes.[8] That is, the excitons that are responsible for this emission band are delocalized over a [Ag(CN)$_2^-$]$_n$ cluster with a large "*n*" value. The HOMO−LUMO gap of this cluster represents the convergence of the band gap of the [Ag(CN)$_2^-$]$_n$ homologues as "*n*" increases. For two-dimensional solids such as dicyanoargentates(I), a good model for such a cluster is a square-planar [Ag(CN)$_2^-$]$_5$ pentamer. Delocalization over five monomer units is easier if the Ag−Ag distances are shorter. Due to the high lattice energies of the alkali halide crystals, we assume that the Ag−Ag distances in the [Ag(CN)$_2^-$]$_n$ species in the doped crystals are the same as the intercationic distances in these crystals. These distances are 4.51 and 4.00 Å in KCl and NaCl, respectively. The corresponding areas of the square-planar pentamers are 40.7 and 32.0 Å^2 in a KCl crystal and a NaCl crystal, respectively. Consequently, the delocalization of a *[Ag(CN)$_2^-$]$_5$ exciton occurs more easily in a NaCl crystal than in a KCl crystal due to the 8.70 Å^2 smaller pentamer area in the former. One should point out that the presence of a [Ag(CN)$_2^-$]$_5$ is very disruptive to the alkali halide lattice, as evidenced by the extremely large Stokes shift associated with band D (Table 1). In fact, we have noticed that doped KCl crystals showing a strong D emission are slightly discolored. Other factors leading to the D emission, which include the irradiation history of the crystal, are under current investigation in our laboratory.

The two types of doped crystals are similar in the individual luminescence bands, despite the large difference in Ag−Ag separations. This is most likely due to excited-state interactions in [Ag(CN)$_2^-$]$_n$ species. Such excited-state interactions have little sensitivity to ground-state metal−metal distances because of exciplex formation.[8] In contrast, the most important factor that affects excited-state interactions in [Ag(CN)$_2^-$]$_n$ is the number of neighboring ions (*n*) and the geometry of the oligomer. Both NaCl and KCl have the same space group; hence, a given [Ag(CN)$_2^-$]$_n$ oligomer has the same geometry in both crystals, which leads to the same luminescence bands, as observed experimentally.

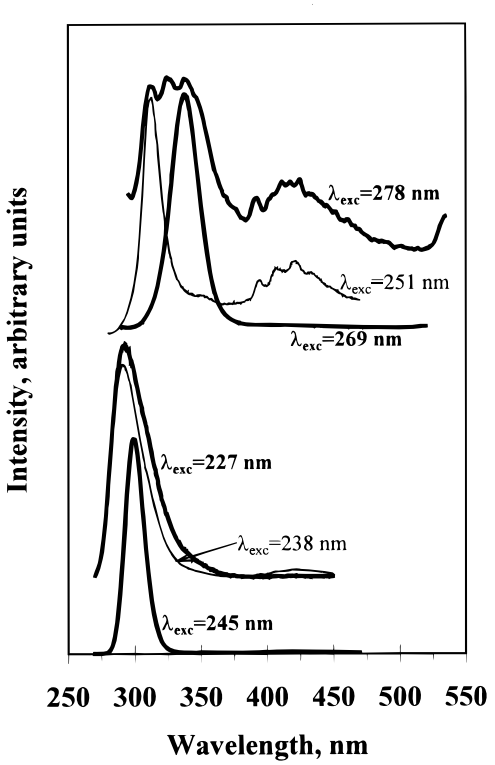

Figure 8. *Fine-tuning* of the dicyanoargentate(I) luminescence obtained by varying the excitation wavelength at 12 K in a single crystal of $[Ag(CN)_2^-]$/KCl.

5. Exciplex Tuning by Temperature Variation. Tuning of the dicyanoargentate(I) luminescence by ~18 000 cm^{-1} has been achieved by a variety of methods such as site-selective excitation,[8] changing the dopant concentration,[25] and in this study by temperature variation in two host crystals. Exciplex tuning in the title crystals can be controlled to show either *coarse tuning* or *fine-tuning*. Coarse tuning is achieved in a single crystal by varying the temperature between 12 K and ambient temperature. For example, Figure 4 shows that the strongest emission is different at different temperatures: B at 12 K, C at 80 K, and A at ambient temperature. Fine-tuning is achieved by varying the excitation wavelength at the same temperature. This controls the profile of the spectrum and the exact position of the emission maximum within the dominant emission band at that temperature. To illustrate, Figure 8 shows the emission spectra of $[Ag(CN)_2^-]$/KCl at 12 K using different excitation wavelengths. Even small changes in the excitation wavelengths lead to significant changes in the emission profile. For example, if it is desired to obtain a narrow emission, one can carefully vary the excitation wavelength in small increments. Figure 8 shows that changing the excitation wavelength from 227 to 238 nm makes band B narrower, but a weak signal due to band C also appears. A further increase in the excitation wavelength to 245 nm makes band B narrower with no interference from band C. If it is desired to obtain a wide range of luminescence energies, one can select an excitation wavelength that leads to more than one luminescence band. For example, Figure 8 shows that changing λ_{exc} from 251 to 269 nm leads to a change in the emission maximum from ~300 to ~330 nm. A further change of λ_{exc} to 278 nm results in the observation of a continuous emission in the ~290−500 nm range (~15 000 cm^{-1} range). These results have important implications for the design of tunable solid-state photonic devices based on materials that have luminescence properties similar to those in the present study. The structured emission shown in Figure 8 for band B is due to the presence of multiple sites with slightly different local symmetries because, like the case for band C, the energy separations between individual peaks comprising the structured emission of band B do not correspond to any of the normal modes of the $[Ag(CN)_2^-]$ ion.

Another interesting property of the crystals studied herein is the observation of strong luminescence at ambient temperature. The strong ambient-temperature luminescence is observed in the UV region of band A with a maximum near 300 nm. Not many UV lasers are available commercially at such short wavelengths. For example, the Nd:YAG laser provides output at 266 nm, but in order to obtain this wavelength, the energy should be quadrupled from 1064 nm (which means diminished intensity at 266 nm). Nitrogen lasers, on the other hand, provide a single line at 337.1 nm, which limits the use of these lasers in the case of species that do not absorb at this wavelength (for example, N_2 lasers are not useful for this study; see Figure 2). Continuum sources such as xenon lamps have very low intensities at wavelengths < 300 nm. Mercury lamps provide useful wavelengths in the UV region, but they are not continuum sources.[47] A photonic device that is based on the luminescence of the mixed crystals in this study would not have these limitations. Such a device would provide strong intensities at ambient temperature in the wavelength range of ~275−325 nm (Figure 4). Moreover, this wavelength range can be *tuned* by considering the ideas in this section as well as those discussed in refs 8 and 25.

It is important to note that dicyanoargentate(I) species display ambient-temperature photoluminescence only in doped crystals such as the title crystals but not in pure crystals such as $Tl[Ag(CN)_2]$ or $K_2Na[Ag(CN)_2]_3$.[37] Self-quenching processes are believed to be the reason for this observation. The excitonic energy is propagated between neighboring $[Ag(CN)_2^-]$ ions within the layered structure of the pure crystals until a crystal defect is reached, which traps the excitation energy and quenches the luminescence. The concentration of the $[Ag(CN)_2^-]$ ions is low in the alkali halide host lattice, which diminishes self-quenching processes in doped crystals.

Conclusions

Remarkably rich luminescence behavior has been observed in $[Ag(CN)_2^-]$/NaCl and $[Ag(CN)_2^-]$/KCl-doped crystals. The luminescence spectra are strongly affected by controlling the temperature, excitation wavelength, and changing the alkali halide host crystal from KCl to NaCl. A strong luminescence thermochromism is observed in all the crystals studied, in which the strongest emission band is vastly different at different temperatures. A reversal of the relative intensities of the high-energy/low-energy emissions has been observed twice in the temperature range of 12 K to ambient temperature. A kinetic model has been proposed to explain the temperature dependence of the luminescence bands. It is concluded that "normal" energy transfer pathways are responsible for the changes between 12 and 80 K, while "back" transfer pathways are responsible for the changes above 80 K. All crystals studied exhibit extremely large tunability of their excited-state energies (by ~18 000 cm^{-1}), which make them promising for technological applications, such as the design of new tunable solid-state photonic devices in the ultraviolet region.

Acknowledgment is made to the donors of the Petroleum Research Fund, administered by the American Chemical Society, for the support of this research.

References and Notes

(1) Jansen, M. *Angew. Chem., Int. Ed. Engl.* **1987**, *26*, 1098.

(2) Kutal, C. *Coord. Chem. Rev.* **1990**, *99*, 213.

(3) Ford, P. C.; Vogler, A. *Acc. Chem. Res.* **1993**, *26*, 220.

(4) (a) De Ahna, H. D.; Hardt, H. D. *Z. Anorg. Allg. Chem.* **1972**, *387*, 61. (b) Hardt, H. D.; Gechnizdjani, H. *Anorg. Allg. Chem.* **1973**, *397*, 23. (c) Hardt, H. D.; Pierre, A. *Anorg. Allg. Chem.* **1973**, *402*, 107. (d) Hardt, H. D.; Pierre, A. *Inorg. Chim. Acta* **1977**, *25*, L59. (e) Hardt, D. D.; Stoll, H. J. *Z. Anorg. Allg. Chem.* **1981**, *480*, 193. Hardt, D. D.; Stoll, H. J. *Z. Anorg. Allg. Chem.* **1981**, *480*, 199.

(5) (a) Kyle, K. R.; Ryu, C. K.; DiBenedetto, J. A.; Ford, P. C. *J. Am. Chem. Soc.* **1991**, *113*, 2954. (b) Kyle, K. R.; DiBenedetto, J. A.; Ford, P. C. *J. Chem. Soc., Chem. Commun.* **1989**, 714. (c) Kyle, K. R.; Ford, P. C. *J. Am. Chem. Soc.* **1989**, *111*, 5005. (d) Kyle, K. R.; Palke, W. E.; Ford, P. C. *Coord. Chem. Rev.* **1990**, *97*, 35. (e) Døssing, A.; Ryu, C. K.; Kudo, S.; Ford, P. C. *J. Am. Chem. Soc.* **1993**, *115*, 5132. (f) Ford, P. C. *Coord. Chem. Rev.* **1994**, *132*, 129. (g) Tran, D.; Ryu, C. K.; Ford, P. C. *Inorg. Chem.* **1994**, *33*, 56. (h) Simon, J. A.; Palke, W. E.; Ford, P. C. *Inorg. Chem.* **1996**, *35*, 6413. (i) Vitale, M.; Palke, W. E.; Ford, P. C. *J. Phys. Chem.* **1992**, *96*, 8329. (j) Vitale, M.; Ryu, C. K.; Palke, W. E.; Ford, P. C. *Inorg. Chem.* **1994**, *33*, 561.

(6) Schmidbaur, H. *Chem. Soc. Rev.* **1995**, 391.

(7) Omary, M. A.; Webb, T. R.; Assefa, Z.; Shankle, G. E.; Patterson, H. H. *Inorg. Chem.* **1998**, *37*, 1380.

(8) Omary, M. A.; Patterson, H. H. *J. Am. Chem. Soc.* **1998**, *120*, 7696.

(9) Omary, M. A.; Patterson, H. H. *Inorg. Chem.* **1998**, *37*, 1060.

(10) Edel, A.; Marnot, P. A.; Sauvage, J. P. *Nouv. J. Chim.* **1984**, *8*, 495.

(11) (a) Zecchina, A.; Bordiga, S.; Palomino, G. T.; Scarano, D.; Lamberti, C.; Salvalaggio, M. *J. Phys. Chem. B.* **1999**, *103*, 3833. (b) Shelef, M. *Chem. Rev.* **1995**, *95*, 209.

(12) (a) Kruglik, G. S.; Skripko, G. A.; Shkadarevich, A. P.; Ermolenko, N. N.; Gorodetskaya, O. G.; Belokon, M. V.; Shagov, A. A.; Zolotareva, L. E. *Opt. Spectrosc. (U.S.S.R.)* **1985**, *59*, 439. (b) Moine, B.; Pedrini, C.; Duloisy, E.; Boutinaud, P.; Parent, C.; Le Flem, G. *J. Physique IV* **1991**, *C7*, 289.

(13) Blonder, R.; Levi, S.; Tao, G.; Ben-Dov, I.; Willner, I. *J. Am. Chem. Soc.* **1997**, *119*, 10467.

(14) Wolf, M. O.; Fox, M. A. *J. Am. Chem. Soc.* **1995**, *117*, 1845.

(15) (a) Roy, P. W.; Elder, R. C.; Tepperman, K. *Metal Based Drugs* **1994**, *1*, 521. (b) Walz, D. T. In *Advances in Inflammation Research*; Otterness, I., Capetola, R., Wond, S., Eds.; Raven Press: New York, 1984; Vol. 7, p 239. (c) Sutton, B. M.; McCusty, E.; Walz, D. T.; DiMartino, M. J. *J. Med. Chem.* **1972**, *15*, 1095.

(16) Mansour, M. A.; Connick, W. B.; Lachicotte, R. J.; Gysling, H. J.; Eisenberg, R. *J. Am. Chem. Soc.* **1998**, *120*, 1329.

(17) (a) Von der Austin, W.; Stolz, H. *J. Phys. Chem. Solids* **1990**, *51*, 765. (b) Hamilton, J. F. *Adv. Phys.* **1988**, *37*, 359. (c) Ueta, M.; Kanzaki, H.; Kabayashi, K.; Toyozawa, Y.; Hanamura, E. *Excitonic Processes in Solids*; Springer: Berlin; 1986; pp 309−69.

(18) Moser, F.; Barkay, N.; Levite, A.; Margalit, E.; Paiss, I.; Sa'ar, A.; Schnitzer, I.; Zur, A.; Katzir, A. *Proc. SPIE* **1990**, *1228*, 128.

(19) (a) Anpo, M.; Matsuoka, M.; Mishima, H.; Yamashita, H. *Res. Chem. Intermed.* **1997**, *23*, 197. (b) Anpo, M.; Matsuoka, M.; Yamashita, H. *Catal. Today* **1997**, *35*, 177. (c) Kanan, S. M.; Omary, M. A.; Patterson, H. H.; Matsuoka, M.; Anpo, M. *J. Phys. Chem. B* **2000**, *104*. 3507.

(20) Köhler, B. U.; Weppner, W.; Jansen, M. *J. Solid State Chem.* **1985**, *57*, 227.

(21) Gruber, H.; Hess, H.; Popitsch, A.; Fischer, A. P. *J. Electrochem. Soc.* **1982**, *129*, 369.

(22) Popitsch, A. *J. Crystallogr. Spectrosc. Res.* **1985**, *15*, 603.

(23) (a) Lowry, T. H.; Schuller-Richardson, K. *Mechanism and Theory in Organic Chemistry*; Harper&Row: New York, 1981; pp 919−925. (b) Turro, N. J. *Modern Molecular Photochemistry*; Benjamin/Cummings: Melano Park, CA, 1978; pp 135−146. (c) Lamola, A. A. In *Energy Transfer and Organic Photochemistry*; Lamola, A. A., Turro, N. J., Eds.; Wiley-Interscience: New York, 1969; pp 54−60. (d) *The Exciplex*; Gordon, M., Ware, W. R., Eds.; Academic Press: New York, 1975. (e) Kopecky, J. *Organic Photochemistry: A Visual Approach*; VCH: New York, 1991; pp 38−40. (f) Michl, J.; Bonacic-Koutecky, V. *Electronic Aspects of Organic Photochemistry*; Wiley: New York, 1990; pp 274−286.

(24) (a) For a recent review see: Horváth, A.; Stevenson, K. L. *Coord Chem. Rev.* **1996**, *153*, 57. (b) The "exciplex bond" refers to an excited-state bond for the exciplex species $*[A_n-B_m]$. An excimer is a subcategory for the general term "exciplex", in which A = B and $n = m = 1$: Omary, M. A.; Patterson, H. H. Electronic Spectroscopy: Luminescence Theory: *Encyclopedia of Spectroscopy & Spectrometry*; Academic Press: London, UK, 2000; pp 1186−1207.

(25) Omary, M. A.; Hall, D. R.; Shankle, G. E.; Siemiarczuck, A.; Patterson, H. H. *J. Phys. Chem. B* **1999**, *103*, 3845.

(26) Melhuish, W. H. *J. Opt. Soc. Am.* **1962**, *52*, 1256.

(27) (a) Following the notation in ref 8 because the $[Ag(CN)_2^-]$ luminescence bands are similar in both $[Ag(CN)_2^-]$/NaCl and $[Ag(CN)_2^-]$/KCl. (b) We have carried out a systematic concentration-dependent luminescence study in solution, in which the concentration is varied gradually over several orders of magnitude (ref 29; Omary, M. A. R.; Omary, M. A.; Patterson, H. H., submitted for publication). The trends obtained for the three doped crystals mentioned here are reproduced in the solution study.

(28) Our recent results show that a similar behavior is obtained in the analogous Au(I) mixed crystals NaCl/$[Au(CN)_2^-]$ and KCl/$[Au(CN)_2^-]$ (see ref 29).

(29) Omary, M. R. Ph.D. Thesis, Graduate School, University of Maine, 1999.

(30) Omary, M. A.; Patterson, H. H.; Shankle, G. *Mol. Cryst. Liq. Cryst.* **1996**, *284*, 399.

(31) (a) Nagle, J. K.; LaCasce, J. H., Jr.; Dolan, P. J., Jr.; Corson, M. R.; Assefa, Z.; Patterson, H. H. *Mol. Cryst. Liq. Cryst.* **1990**, *181*, 359. (b) Patterson, H. H.; Roper, G.; Biscoe, J.; Ludi, A.; Blom, N. *J. Lumin.* **1984**, *31/32*, 555. (c) Markert, J. T.; Blom, N.; Roper, G.; Perregaux, A. D.; Nagasundaram, N.; Corson, M. R.; Ludi, A.; Nagle, J. K.; Patterson, H. H. *Chem. Phys. Lett.* **1985**, *118*, 258. (d) LaCasce, J. H., Jr.; Turner, W. A.; Corson, M. R.; Dolan, P. J., Jr.; Nagle, J. K. *Chem. Phys.* **1987**, *118*, 289.

(32) (a) Yersin, H.; Gliemann, G. *Ann. N.Y. Acad. Sci.* **1978**, *313*, 539. (b) Gliemann, G.; Yersin, H. *Struct. Bonding* **1985**, *62*, 87.

(33) Yersin, H.; Riedl, U. *Inorg. Chem.* **1995**, *34*, 1642.

(34) Connick, W. B.; Henling, L. M.; Marsh, R. E.; Gray, H. B. *Inorg. Chem.* **1996**, *35*, 6261.

(35) Omary, M.; Patterson, H. H.; Eckert, J.; Jacubinas, R. Unpublished results.

(36) Larochelle, C. L.; Omary, M. A.; Patterson, H. H.; Fischer, P.; Fauth, F.; Allenspach, P.; Lucas, B.; Pattison, P. *Solid State Commun.* **2000**, *114*, 155.

(37) Omary, M. A. Ph.D. Thesis, Graduate School, University of Maine, 1997.

(38) Kambli, U.; Güdel, H. U. *Inorg. Chem.* **1984**, *23*, 3479.

(39) Omary, M. A. R.; Larochelle, C. L.; Patterson, H. H. Tunable Energy Transfer from Dicyanoaurate(I) and Dicyanoargentate(I) Donor Ions to Tb(III) Acceptor Ions in Pure Crystals, submitted for publication.

(40) This assumption is also reasonable because of the presence of isoluminescent points between bands A and B as well as between C and D (for example note the two isoluminescent points at ca. 307 and 322 nm between bands A and B in Figure 4). This indicates equilibrium between the two excitons responsible for these bands.

(41) Freed, K. F.; Jortner, J. *J. Chem. Phys.* **1970**, *52*, 6272.

(42) Riesen, H.; Güdel, H. U. *Chem. Phys. Lett.* **1987**, *133*, 429.

(43) Yersin, H.; Gallhuber, E.; Hensler, G. *Chem. Phys. Lett.* **1987**, *140*, 157.

(44) (a) Zink, J. I.; Shin, K. S. K. *Molecular Distortions in Excited Electronic States Determined from Electronic and Resonance Raman Spectroscopy*. In *Advances in Photochemistry*; Volman, D. H., Hammond, G. S., Neckers, D. C., Eds.; Wiley: New York, 1991; Vol. 16. (b) Tutt, L.; Zink, J. I. *J. Am. Chem. Soc.* **1986**, *108*, 5830. (c) Preston, D. M.; Guentner, W.; Lechner, A.; Gliemann, G.; Zink, J. I. *J. Am. Chem. Soc.* **1988**, *110*, 5628. (d) Hollingsworth, G.; Shin, K. S. K.; Zink, J. I. *Inorg. Chem.* **1990**, *29*, 2501.

(45) (a) Wong, P. T. T. *J. Chem. Phys.* **1979**, *70*, 456. (b) Bottger, G. L.; *Spectrochim. Acta Part A* **1968**, *24*, 1821. (c) Loehr, T. M.; Long, T. V., II. *J. Chem. Phys.* **1970**, *53*, 4182. (d) Chadwick, B. M.; Frankiss, S. G. *J. Mol. Struct.* **1968**, *2*, 281.

(46) (a) Gebhardt, W.; Kühnert, H. *Phys. Lett.* **1964**, *11*, 15. (b) For a review see: Markham, J. J. *F-Centers in Alkali Halides*; Academic Press: New York and London, 1966; Chapter X.

(47) For a discussion of light sources in optical instruments, see: Skoog, D. A.; Holler, F. J.; Nieman, T. A. *Principles of Instrumental Analysis*, 5th ed.; Harcourt Brace: Philadelphia, 1998.